available at www.sciencedirect.com

ScienceDirect

journal homepage: www.elsevier.com/locate/jmbbm

Research paper

Improved fatigue life of acrylic bone cements reinforced with zirconia fibers

Robert J. Kane[a], *Weimin Yue*[b], *James J. Mason*[b], *Ryan K. Roeder*[a,*]

[a] *Department of Aerospace and Mechanical Engineering, Bioengineering Graduate Program, University of Notre Dame, Notre Dame, IN 46556, United States*

[b] *OrthoX (formerly Granger Engineering, LLC), Granger, IN 46530, United States*

ARTICLE INFO

Article history:
Received 29 March 2010
Received in revised form
19 May 2010
Accepted 29 May 2010
Published online 8 June 2010

Keywords:
Acrylic bone cement
Fatigue
Fiber
Implant fixation
Poly(methyl methacrylate)
Zirconia

ABSTRACT

Poly(methyl methacrylate) (PMMA) bone cements have a long and successful history of use for implant fixation, but suffer from a relatively low fracture and fatigue resistance which can result in failure of the cement and the implant. Fiber or particulate reinforcement has been used to improve mechanical properties, but typically at the expense of the pre-cured cement viscosity, which is critical for successful integration with peri-implant bone tissue. Therefore, the objective of this study was to investigate the effects of zirconia fiber reinforcement on the fatigue life of acrylic bone cements while maintaining a relatively low pre-cured cement viscosity. Sintered straight or variable diameter fibers (VDFs) were added to a PMMA cement and tested in fully reversed uniaxial fatigue until failure. The mean fatigue life of cements reinforced with 15 and 20 vol% straight zirconia fibers was significantly increased by ~40-fold, on average, compared to a commercial benchmark (Osteobond^{TM}) and cements reinforced with 0–10 vol% straight zirconia fibers. The mean fatigue life of a cement reinforced with 10 vol% VDFs was an order of magnitude greater than the same cement reinforced with 10 vol% straight fibers. The time-dependent viscosity of cements reinforced with 10 and 15 vol% straight fibers was comparable to the commercial benchmark during curing. Therefore, the addition of relatively small amounts of straight and variable diameter zirconia fibers was able to substantially improve the fatigue resistance of acrylic bone cement while exhibiting similar handling characteristics compared to current commercial products.

1. Introduction

Poly(methyl methacrylate) (PMMA) cements have been the method of choice for affixing total joint replacements to peri-implant bone tissue ever since the pioneering efforts by Charnley and others in the 1960s (Charnley, 1960; Davies et al., 1987). Cement fixation of the femoral component is used in approximately one-half of all total hip arthroplasties and has proved to be an extremely effective technique with a 90% success rate after 15 years (Murray et al., 1995). However, increased life expectancy and the decreasing age of implant

* *Corresponding address:* Department of Aerospace and Mechanical Engineering, University of Notre Dame, 148 Multidisciplinary Research Building, Notre Dame, IN 46556, United States. Tel.: +1 574 631 7003; fax: +1 574 631 2144.
E-mail address: rroeder@nd.edu (R.K. Roeder).

1751-6161/$ - see front matter © 2010 Elsevier Ltd. All rights reserved.
doi:10.1016/j.jmbbm.2010.05.007

recipients suggest a clinical need for further improvements in the implant lifetime. Cemented implants can fail through a variety of mechanisms, including inflammation caused by wear particles, micro-motion at the bone–cement interface, and fracture of the cement mantle (Bauer and Schils, 1999). Thus, the fracture and fatigue resistance of PMMA bone cements is a significant factor affecting implant failure.

A wide variety of approaches have been used to improve the mechanical properties of PMMA bone cements (Lewis, 1997), including the addition of a reinforcing particle or fiber to increase cement strength, stiffness, and toughness (Lewis, 2003, 2008). Numerous reinforcements have been examined in fatigue, including carbon fibers (Martin et al., 1980; Pilliar et al., 1976; Robinson et al., 1981), hydroxyapatite particles (Harper et al., 1995, 2000) or fibers (Matsuda et al., 2004), PMMA fibers (Gilbert et al., 1995), stainless steel fibers (Kotha et al., 2004, 2006a), titanium fibers (Kotha et al., 2006b; Topoleski et al., 1995), and zirconia particles (Harper and Bonfield, 2000) or fibers (Kotha et al., 2009; Zhou et al., 2009), among others. Regardless of the reinforcement composition, short fibers or equiaxed particles are usually added to the cement at 1–20 vol%. Most studies have reported improved fatigue properties as a result of this reinforcement (Lewis, 2003). However, most reinforced cements also exhibit a significantly higher dough-stage viscosity, leading to difficulty in obtaining a reliable bone–cement interface (Lewis, 2008). Moreover, a high viscosity limits handling and the addition of higher reinforcement fractions.

Reinforced cements have also been limited by poor adhesion between the PMMA matrix and reinforcement fibers or particles. Therefore, recent studies have attempted to improve the interfacial strength or resistance to fiber pullout either chemically, using coupling agents (Harper et al., 2000; Kotha et al., 2006a,b; Lewis, 2008), or mechanically, using variable diameter fibers (VDFs) (Zhou et al., 2005, 2009). VDFs improve stress transfer by mechanical interlocking (Zhu and Beyerlein, 2002), analogous to fastening with a screw rather than a nail. In a preliminary study, cements reinforced with VDFs exhibited increased tensile strength and fatigue life compared to conventional straight fibers at low reinforcement fractions, up to 10 vol% (Zhou et al., 2009).

The objective of this study was to investigate the fatigue life of PMMA bone cements reinforced with straight or variable diameter zirconia fibers compared to a commercial benchmark. Moreover, the PMMA cement composition was tailored such that the pre-cured viscosity of reinforced cements exhibited similar handling characteristics compared to the commercial benchmark.

2. Materials and methods

2.1. *Cement preparation*

Zirconia fibers were prepared by Advanced Cerametrics Inc. (Lambertville, NJ), using the viscous suspension spinning process (VSSP) and sintering, as described elsewhere (Cass et al., 1998, 2003). Straight fibers were approximately 100 μm in length and 20 μm in diameter, on average (Fig. 1(a)). VDFs were approximately 750 μm in length, with a maximum diameter of 200 μm and minimum diameter of 100 μm (cf. Zhou et al., 2009). The larger size of VDFs was dictated by processing constraints, but the approximate aspect ratio (ratio of the length and mean width) was similar to the straight fibers. Both types of fibers were polycrystalline with a submicron grain size and surface roughness (Fig. 1(b)).

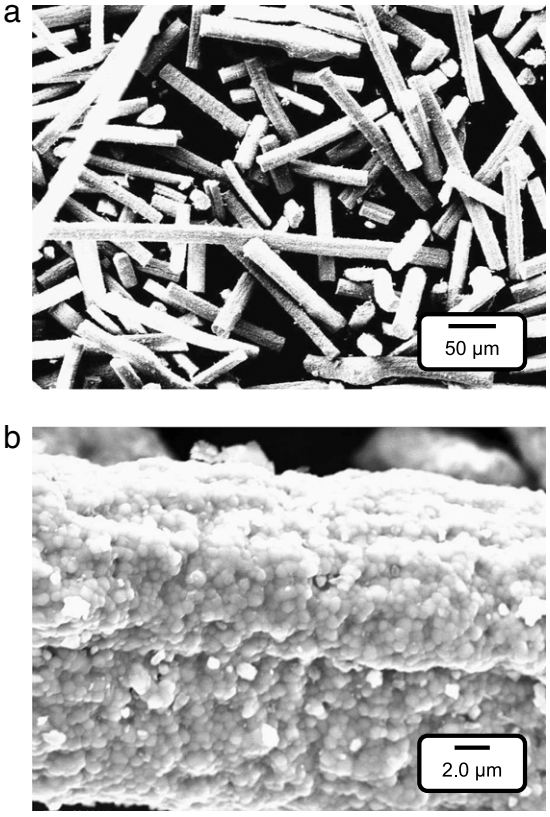

Fig. 1 – Scanning electron micrographs showing the (a) fiber morphology, and (b) submicron grain size and surface roughness of as-prepared polycrystalline, straight zirconia fibers.

Acrylic powder beads comprised a poly(methyl methacrylate-*co*-styrene) copolymer with 0.85 wt% residual benzoyl peroxide (BPO) as a polymerization initiator. The mean bead size was 37 μm with a maximum bead size of 150 μm. Cements reinforced with 15 vol% straight fibers were also prepared using acrylic beads with a mean size of 26 and 48 μm for comparison. The powder component was provided without a radiopacifier (e.g., barium sulfate) due to reinforcement by zirconia fibers which also provided radiopacity. Zirconia reinforcements have been used as a radiopacifier in a number of commercial cements (Harper and Bonfield, 2000; Lewis, 1997, 2003). The liquid component was composed of methyl methacrylate (MMA) monomer, with 0.725 vol% *N*, *N*-dimethyl-*p*-toluidine (DMPT) as a polymerization accelerator and 60 ± 10 ppm hydroquinone as a stabilizer.

The acrylic cement was formulated for decreased viscosity prior to the addition of 5, 10, 15, and 20 vol% straight fibers or 10 vol% VDFs. The powder and liquid components were vacuum mixed (~70 kPa) at a powder-to-liquid ratio of 0.9 g/ml following standard clinical methods, except that zirconia fibers were added at the same time as the

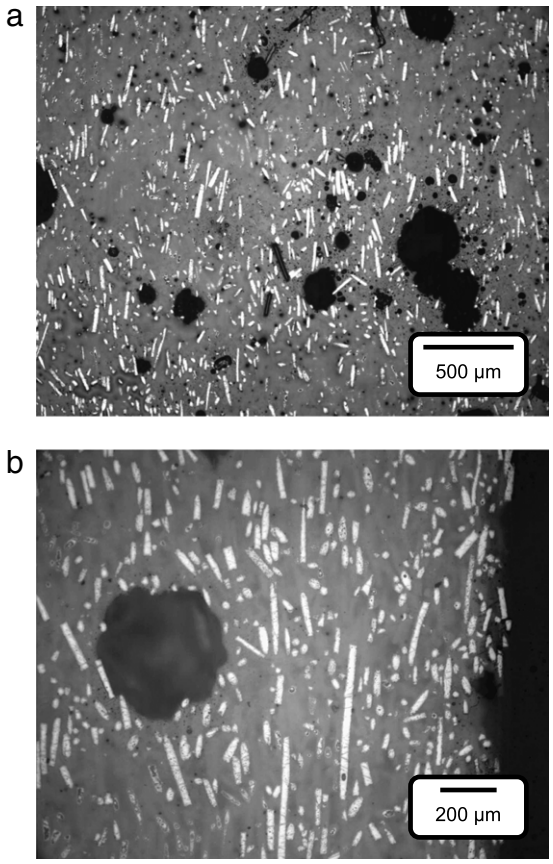

Fig. 2 – Optical micrographs of polished longitudinal cross-sections for a run-out specimen (10 million cycles without failure) from the cement reinforced with 15 vol% straight fibers showing (a) porosity and (b) a region near the free surface. Note the relative alignment of zirconia fibers in the vertical direction corresponding to cement injection and uniaxial loading.

PMMA powder. Note that all aspects of the above cement composition, except the powder-to-liquid ratio and zirconia fiber reinforcements, were within the range of commercial cement compositions (Harper and Bonfield, 2000; Lewis, 1997, 2003). The liquid-to-powder ratio was decreased due to the effective substitution of zirconia fibers for PMMA powder, but was within the range employed for hypodermic injection of cements in vertebroplasty (Lewis, 2009). Reinforced cements were compared against the same PMMA formulation without reinforcement as a control, and a commercially available cement (Osteobond^{TM}, Zimmer Inc., Warsaw, IN) as a clinical benchmark.

The pre-cured cement viscosity was measured using a cone and plate viscometer (DV-E, Brookfield Engineering, Middleboro, MA) at 2.5 rpm and 20.5 °C. Measurements were taken at 30 s intervals beginning immediately after mixing the monomer, powder, and fibers.

Control and zirconia fiber reinforced PMMA cement test specimens were prepared by injection into silicone molds, resulting in fiber alignment along the direction of loading for fatigue tests (Fig. 2). Specimen dimensions followed ASTM F2118-03 with a gage section 5 mm in diameter and 25 mm in length, and a 5 mm chamfer transitioning to 10 mm diameter grip sections (ASTM, 2003). Surface imperfections, such as the mold parting line, were removed by lightly sanding the gage section of each specimen with 400, 800, and 1200 grit SiC paper.

2.2. *Fatigue testing and analysis*

Fatigue testing utilized the Harris protocol (Davies et al., 1987), as outlined in ASTM (2003). After equilibrating for several days in saline, specimens were loaded to failure under fully reversed uniaxial tension–compression with a sinusoidal waveform at 10 Hz to a maximum stress of ±15 MPa using a servohydraulic load frame (Model 810, MTS Systems Corp., Eden Prairie, MN). All tests were conducted in phosphate buffered saline (pH = 7.4) at 37 °C to simulate physiological conditions. The secant modulus was measured from load–displacement hysteresis loops collected throughout the test. The relative modulus degradation, E/E_0, was measured as the ratio of the secant modulus at a given number of loading cycles by the initial secant modulus, measured at the 50th loading cycle. Differences in the initial secant modulus were compared by one-way analysis of variance (ANOVA) (JMP 5.1, SAS Institute, Inc., Cary, NC). Post hoc comparisons were performed using Tukey's HSD test with a level of significance of 0.05. Differences in the relative modulus degradation were examined by comparing the median specimen for each experimental group based on the fatigue life.

The fatigue life was measured as the total number of loading cycles at failure. A log transform was used to provide a normal distribution for the comparison of experimental groups by one-way ANOVA (ASTM, 2003). Post hoc comparisons were performed using Tukey's HSD test with a level of significance of 0.05. Each experimental group initially included five specimens, with the exception that the commercial control group included two additional specimens. All specimens for cements reinforced with 15 vol% straight zirconia fibers were grouped together as differences between groups with a mean acrylic bead size of 26, 37 and 48 μm were not statistically significant ($p = 0.86$, ANOVA). Groups for cements reinforced with 0, 10 and 15 vol% straight zirconia fibers lost one specimen each due to instrument malfunction during the test or the presence of a large pore (>1 mm) within the gage section. Two specimens for cements reinforced with 15 vol% straight zirconia fibers did not fail after 10 million cycles (run-out) and were therefore not included in the mean fatigue life or Weibull analysis.

The probability of failure, P_f, for specimens from each experimental group was estimated using a two-parameter Weibull distribution as,

$$P_f = 1 - \exp[-(N_f/\beta)^m] \quad (1)$$

where N_f is the number of cycles to failure, β is the scale parameter or Weibull characteristic fatigue life (at $P_f = 0.632$), and m is the shape parameter or Weibull modulus. The scale and shape parameters were determined by mean rank regression, plotting the Weibull parameter, $\log(-\log(1 - P_f))$, using mean rank values for P_f, versus log (N_f) and fitting by linear least-squares regression.

$$\log(-\log(1 - P_f)) = m \cdot \log(N_f) - m \cdot \log(\beta). \quad (2)$$

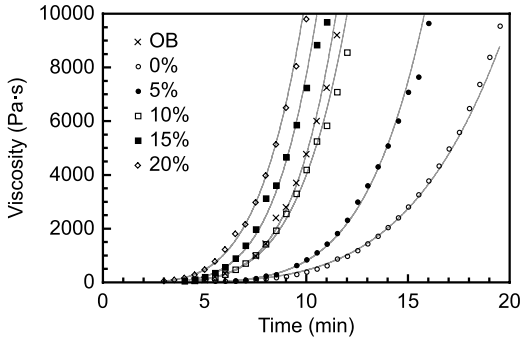

Fig. 3 – The pre-cured cement viscosity of a commercial benchmark (Osteobond™, OB) and cements containing 0, 5, 10, 15 and 20 vol% straight zirconia fibers.

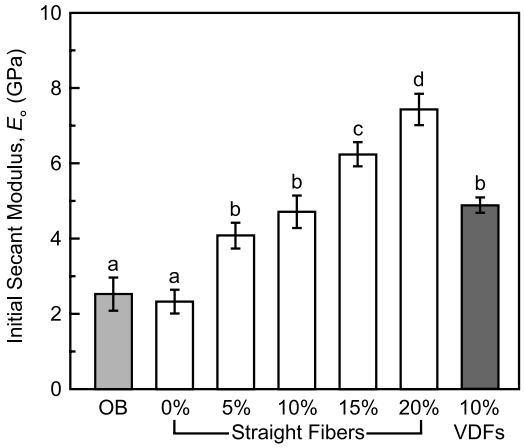

Fig. 4 – The mean initial secant modulus of specimens prepared from a commercial benchmark (Osteobond™, OB) and cements containing 0, 5, 10, 15 and 20 vol% straight zirconia fibers and 10 vol% variable diameter zirconia fibers (VDFs). Error bars span one standard deviation. Groups not connected by the same letter exhibited a statistically significant difference ($p < 0.05$, Tukey's HSD test). Secant moduli were measured from cyclic hysteresis loops using actuator displacements. Therefore, relative comparisons should be emphasized rather than absolute magnitudes, which are expected to be underestimated compared to elastic moduli measured from static tensile tests using an extensometer.

Scale and shape parameters for each regression were compared using analysis of covariance (ANCOVA) with a level of significance of 0.05.

Failure surfaces from representative specimens were coated with Au–Pd by sputter deposition and imaged using scanning electron microscopy (Evo 50, LEO Microscopy Ltd, Cambridge, UK) at an accelerating voltage of 15 kV and a working distance of 7–10 mm. Additionally, a specimen reinforced with 15 vol% straight zirconia fibers, and loaded to 10 million cycles without failure (run-out), was sectioned longitudinally with a low speed diamond wafer saw, polished with a series of SiC and diamond abrasives, and imaged using reflected light microscopy (Eclipse ME600, Nikon Instruments Inc., Melville, NY) in order to examine for the presence of microcracks or fatigue damage.

3. Results

The viscosity of the PMMA bone cement without reinforcement was much lower than the commercial benchmark (Osteobond™) for a given time period, such that the addition of fiber reinforcement increased the viscosity toward that of the commercial benchmark (Fig. 3). Therefore, the time-dependent viscosity of cements reinforced with 10 and 15 vol% straight zirconia fibers was similar to that of the commercial benchmark (Fig. 3), and thus exhibited similar handling characteristics.

The initial secant modulus, E_o, increased with increased zirconia fiber reinforcement ($p < 0.001$, ANOVA), as expected (Fig. 4). The commercial control and unreinforced cement did not exhibit a statistically significant difference in the initial secant modulus. The initial secant modulus of cements reinforced with 10 vol% straight zirconia fibers and VDFs was also not statistically different.

The mean fatigue life of cements reinforced with 15 and 20 vol% straight zirconia fibers was significantly greater ($p < 0.05$, Tukey's HSD test) than the commercial benchmark and cements reinforced with 0–10 vol% straight zirconia fibers (Fig. 5). For example, the mean fatigue life of the cement reinforced with 15 vol% straight zirconia fibers was 67 times greater than the commercial benchmark and 22 times greater than the same cement formulation without fiber reinforcement. Note that these differences are conservative because the mean fatigue life reported for the cement reinforced with 15 vol% straight zirconia fibers did not include two specimens which did not fail after 10 million cycles (run-out). There were no statistically significant differences in the mean fatigue life between the commercial benchmark and cements reinforced with 0–10 vol% straight zirconia fibers, as well as between cements reinforced with 15 and 20 vol% straight fibers.

The mean fatigue life of the cement reinforced with 10 vol% VDFs was significantly greater ($p < 0.05$, Tukey's HSD

Table 1 – Summary of the Weibull distribution shape parameter (Weibull modulus), scale parameter (Weibull characteristic fatigue life), and correlation coefficient determined by mean rank regression using Eq. (2), for specimens prepared from a commercial benchmark (Osteobond™, OB) and cements containing 0, 5, 10, 15 and 20 vol% straight zirconia fibers and 10 vol% variable diameter zirconia fibers (VDFs). Shape and scale parameters not connected by the same superscript letter exhibited statistically significant differences between the regression parameters ($p < 0.05$, ANCOVA).

Cement	Shape parameter, m	Scale parameter, β (cycles)	R^2
OB	1.93^{a}	$7.62{\cdot}10^{4\,a}$	0.97
0 vol%	0.58^{b}	$2.46{\cdot}10^{5\,b}$	0.98
5 vol%	$1.46^{c,d}$	$7.08{\cdot}10^{4\,a}$	0.95
10 vol%	2.35^{a}	$1.34{\cdot}10^{5\,b}$	0.90
15 vol%	$1.77^{a,c}$	$5.09{\cdot}10^{6\,c}$	0.98
20 vol%	1.15^{d}	$3.63{\cdot}10^{6\,d}$	0.98
10 vol% VDFs	0.80^{b}	$1.20{\cdot}10^{6\,b}$	0.95

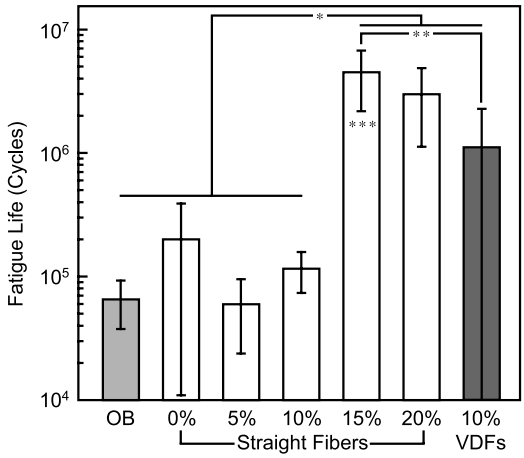

Fig. 5 – The mean fatigue life of specimens prepared from a commercial benchmark (Osteobond^{TM}, OB) and cements containing 0, 5, 10, 15 and 20 vol% straight zirconia fibers and 10 vol% variable diameter zirconia fibers (VDFs). Error bars span one standard deviation. The mean fatigue life of cements reinforced with 15 or 20 vol% straight fibers and 10 vol% VDFs was significantly greater than the commercial benchmark and cements reinforced with 0–10 vol% straight fibers (*$p < 0.05$, Tukey's HSD test), and the mean fatigue life of cement reinforced with 15 vol% straight fibers was also significantly greater than the cement reinforced with 10 vol% VDFs ($p < 0.05$, Tukey's HSD test). ***Note that data plotted for the cement reinforced with 15 vol% straight zirconia fibers does not include two specimens that did not fail after 10 million cycles (run-out).**

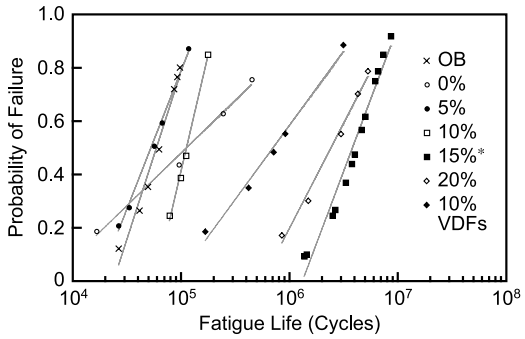

Fig. 6 – Weibull probability of failure analysis for specimens prepared from a commercial benchmark (Osteobond^{TM}, OB) and cements containing 0, 5, 10, 15 and 20 vol% straight zirconia fibers and 10 vol% variable diameter zirconia fibers (VDFs). *Note that data plotted for the cement reinforced with 15 vol% straight zirconia fibers does not include two specimens that did not fail after 10 million cycles (run-out). The plotted data points were fit by linear least-squares regression in order to aid visual comparison. The Weibull distribution shape and scale parameters are tabulated in Table 1.

test) than the cement reinforced with 10 vol% straight fibers (Fig. 5). The mean fatigue life of the cement reinforced with 10 vol% VDFs was significantly lower ($p < 0.05$, Tukey's HSD test) than the cement reinforced with 15 vol% straight fibers, but was not significantly different from the cement reinforced with 20 vol% straight fibers.

The Weibull characteristic fatigue life (N_f at $P_f = 0.632$ in Fig. 6) for cements in each group exhibited a similar trend, 15 vol% > 20 vol% > 10 vol% VDFs ≫ 0 vol% ≈ 10 vol% > OB ≈ 5 vol% (Table 1), compared to the mean fatigue life (Fig. 5). The commercial benchmark and cements reinforced with 10 and 15 vol% straight fibers exhibited the greatest Weibull modulus, which was not significantly different between these groups (Table 1), indicative of a relatively narrow distribution in fatigue lifetimes (Fig. 6).

All specimens generally exhibited <5% degradation in secant modulus prior to failure. Control groups and cements reinforced with lower levels of fiber reinforcement qualitatively exhibited a greater rate of secant modulus degradation before failure (Fig. 7(a)). SEM micrographs corroborated relatively smooth failure surfaces in control groups and increased tortuosity with increased levels of fiber reinforcement (Fig. 8). Moreover, microscopic examination of a run-out specimen (10 million cycles without failure) from the cement reinforced with 15 vol% straight fibers revealed no evidence of microcracks or fatigue cracks, even in regions of higher relative porosity and near specimen edges (Fig. 2). Cements reinforced with equal fractions of straight fibers

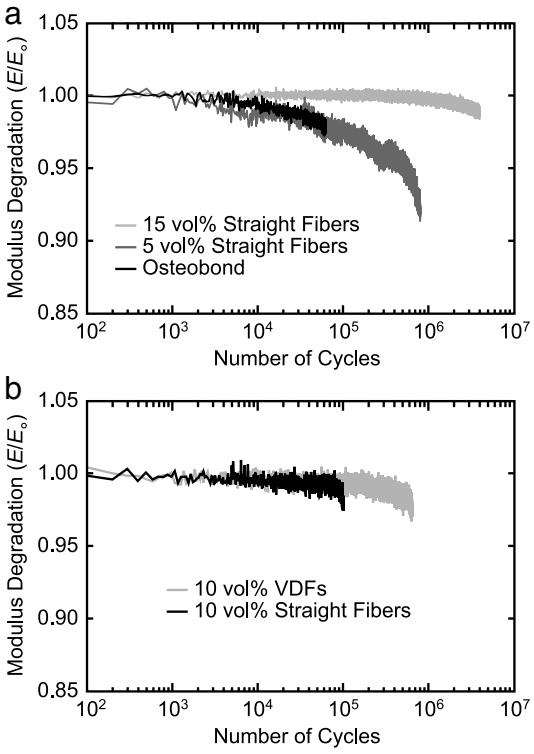

Fig. 7 – The relative secant modulus degradation during fatigue qualitatively comparing the behavior of (a) the commercial benchmark (Osteobond^{TM}) and cements reinforced with low versus high levels of straight zirconia fibers, and (b) cements reinforced with straight versus variable diameter fibers at the same reinforcement level. Data is plotted for specimens that exhibited the median fatigue life in each group.

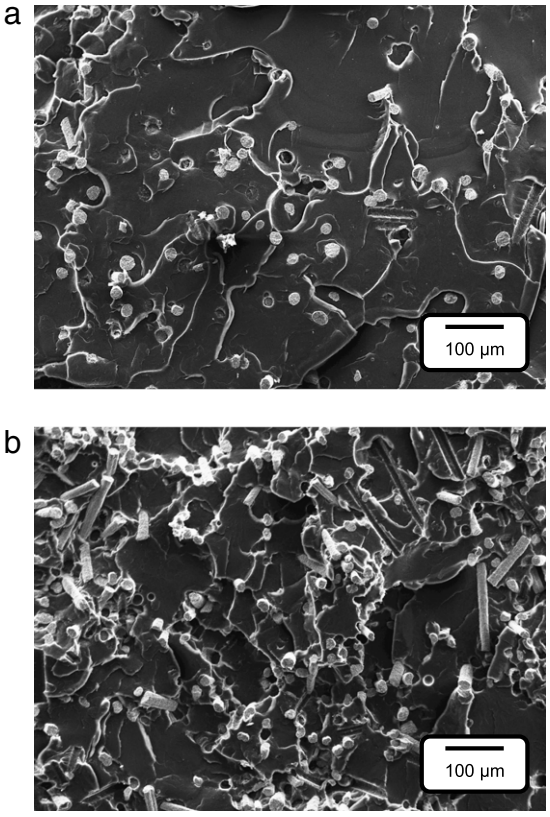

Fig. 8 – Scanning electron micrographs showing representative fatigue failure surfaces for specimens prepared with cements containing (a) 5 vol% and (b) 15 vol% straight zirconia fibers.

versus VDFs exhibited no qualitative differences in the rate of secant modulus degradation (Fig. 7(b)).

4. Discussion

The fatigue life of cements reinforced with 15 and 20 vol% straight zirconia fibers was significantly greater than the same cement formulation with 0–10 vol% straight fibers and the commercial benchmark (Fig. 5). These improvements are expected to translate into improved fatigue resistance of the cement mantle, which may lead to extended life for cemented implants. Zirconia fiber reinforcement increased the fatigue resistance by slowing fatigue crack propagation through energy dissipation mechanisms such as crack deflection, bridging and pullout (Topoleski et al., 1995; Zhou et al., 2009). This explanation was supported by the relatively low secant modulus degradation observed over most of the fatigue life for cements with higher levels of fiber reinforcement (Fig. 5), combined with the increased tortuosity of failure surfaces due to crack deflection, bridging and pullout of fibers (Fig. 8). Low levels of fiber reinforcement were observed in this study to be ineffective at significantly improving the fatigue resistance, most likely due to the enhanced propensity for crack initiation at the fiber/matrix interface. The dramatic increase in fatigue life from 10 to 15 vol% straight fibers (Fig. 5) suggests that a critical mean spacing of fibers was achieved for inhibiting crack propagation and/or interacting with a microcrack prior to reaching a critical size, and should be investigated further.

VDF fibers were also shown to significantly improve the fatigue life compared to straight fibers at the same level of reinforcement (Fig. 5), though it must be noted that processing constraints dictated that VDFs were of greater length but similar aspect ratio compared to straight fibers. VDFs provided greater resistance to pullout due to mechanical interlock with the matrix, as undulations on the fiber surface were mechanically analogous to the threads of a screw (Zhou et al., 2005; Zhu and Beyerlein, 2002). On the other hand, the VDF-reinforced cement exhibited a lower Weibull modulus compared the same level of straight fibers (Table 1, Fig. 6), indicating greater variability in the fatigue life. This greater variability may have been caused by the greater size of VDFs or variability in the VDFs themselves. Finally, the cost of manufacturing VDFs would certainly be greater than straight fibers. Thus, for the above reasons, the cement reinforced with 15 vol% straight zirconia fibers was considered to have the most commercial and clinical potential, though VDFs provided compelling reasons for further study. Interestingly, micrographs of the surface of as-prepared straight zirconia fibers (Fig. 1(b)) and failure surfaces of cements reinforced with straight zirconia fibers (Fig. 8) revealed a polycrystalline surface roughness that likely contributed to enhancing the fiber-matrix interfacial strength in a manner similar to the VDFs.

A previous study investigated the fatigue life of cements reinforced with 2 and 10 vol% straight and variable diameter zirconia fibers (Zhou et al., 2009). The cement formulation was similar except that straight fibers were prepared to have a much greater size (6.35 mm in length) and aspect ratio (~50), but a lower surface roughness, compared to those in this study. Therefore, the mean fatigue life of the cements reinforced with 10 vol% straight fibers was not significantly different ($p > 0.05$ Tukey's HSD) between studies after including data from the prior study in the statistical analysis for all groups in this study. Moreover, the mean fatigue life of the cements reinforced with 10 vol% VDFs from each study were not significantly different ($p > 0.05$ Tukey's HSD), as expected.

The use of Osteobond™ (Zimmer, Inc., Warsaw, IN) as the commercial benchmark in this study was supported by the results of a prior study comparing the tensile fatigue properties of ten commercial acrylic bone cements (Harper and Bonfield, 2000). The Weibull median fatigue life of Osteobond™ was significantly lower than one cement (Palacos® R, Heraeus Kulzer GmbH, Hanau, Germany), not significantly different from four cements (including Surgical Simplex® P, Stryker Orthopaedics, Mahway, NJ), and significantly greater than four cements. Osteobond™, Surgical Simplex® P, and Palacos® R are considered low, medium and high viscosity cements, respectively (Lewis, 1997, 2003). Therefore, cements reinforced with 15 and 20 vol% straight zirconia fibers in this study are low to medium viscosity cements (Fig. 3).

This study was not without several limitations. For the Weibull analysis, the number of specimens per experimental group was small for all groups except cements reinforced

with 15 vol% straight fibers. Therefore, conclusions from the Weibull analysis emphasized relative comparisons, rather than absolute magnitudes.

A single stress level of 15 MPa was employed for fully reversed uniaxial tension–compression fatigue based upon long-standing industry practice (Davies et al., 1987) and, more recently, the highest stress level recommended in ASTM (2003). For comparison, the maximum tensile principal stress in the cement mantle around the femoral component in total hip arthroplasty was reported to be 7.6 and 38 MPa for a bonded and unbonded, respectively, cement–stem interface (Lennon and Prendergrast, 2001). Even in the debonded case, nearly 80% of the cement volume experienced tensile principal stress less than 3 MPa. Higher or lower stress levels would certainly decrease or increase, respectively, the fatigue life, but the relative effects between different cements in this study are not yet known.

The preparation of test specimens resulted in apparent fiber alignment along the direction of loading during fatigue (Fig. 2), which would be expected to enhance the fatigue strength compared to randomly oriented fibers. This fiber alignment may or may not reflect conditions in cement mantle after following surgical procedures for implantation. Future studies could readily quantify the fiber orientation distribution using stereological measurements on two-dimensional sections (Bay and Tucker, 1992; Toll and Andersson, 1991) or three-dimensional micro-computed tomography (Shen et al., 2004). Effects of a fiber orientation distribution on static mechanical properties have been modeled using micromechanics (Camacho et al., 1990; Yue and Roeder, 2006) or finite element analysis (Lusti et al., 2002), but modeling the effects on fatigue life would be more complex.

The porosity and pore size distribution were not measured. The mean fatigue life for the unreinforced cement was not different than the commercial control (Fig. 5), suggesting there was little or no difference in the mean porosity or pore size. However, the Weibull modulus of the unreinforced cement was significantly lower than the commercial control (Table 1, Fig. 6), suggesting greater variability in the porosity or pore size. The porosity evident in SEM micrographs of failure surfaces for one representative specimen from each group was measured to range from 5%–12% using standard stereological methods, which was within the range reported for commercial cements (Lewis, 1997). Volumetric measurements of the porosity and pore size distribution by micro-CT were beyond the scope of the present study, but would be interesting in light of recent studies demonstrating the ability to account for experimental variability in the fatigue life of acrylic bone cement (Hoey and Taylor, 2009a,b). Zirconia fiber reinforcement was expected to mitigate the negative effects of porosity. However, the addition of zirconia fibers may have also decreased the level of porosity, the mean pore size, and/or the pore size distribution by displacing a volume fraction of the polymer phase and inhibiting the coalescence of pores during mixing and curing.

5. Conclusions

The mean fatigue life of cements reinforced with 15 and 20 vol% straight zirconia fibers was significantly increased by ~40-fold, on average, compared to a commercial benchmark (Osteobond^{TM}) and cements reinforced with 0–10 vol% straight zirconia fibers. The mean fatigue life of a cement reinforced with 10 vol% VDFs was an order of magnitude greater than the same cement reinforced with 10 vol% straight fibers. The time-dependent viscosity of cements reinforced with 10 and 15 vol% straight fibers was comparable to the commercial benchmark during curing. Therefore, the addition of relatively small amounts of straight and variable diameter zirconia fibers was able to substantially improve the fatigue resistance of acrylic bone cement while exhibiting similar handling characteristics compared to current commercial products.

Acknowledgements

This research was supported by the National Science Foundation, Division of Industrial Innovation and Partnerships (NSF IIP-0548663), as a Small Business Technology Transfer Research (STTR) Phase II project, and matching funds from the State of Indiana, 21st Century Research and Technology Fund.

REFERENCES

ASTM Standard F2118-03, 2003. Standard test method for constant amplitude of force controlled fatigue testing of acrylic bone cement materials. American Society for Testing and Materials, West Conshohocken, PA.

Bauer, T., Schils, J., 1999. The pathology of total joint arthroplasty. II. Mechanisms of implant failure. Skeletal Radiol. 28 (9), 483–497.

Bay, R.S., Tucker III, C.L., 1992. Stereological measurement and error estimates for three-dimensional fiber orientation. Polym. Eng. Sci. 32 (4), 240–253.

Camacho, C.W., Tucker III, C.L., Yalvaç, S., McGee, R.L., 1990. Stiffness and thermal expansion predictions for hybrid short fiber composites. Polym. Compos. 11 (2), 229–239.

Cass, R.B., Khan, A., Mohammadi, F., 2003. Innovative ceramic-fiber technology energizes advanced cerametrics. Am. Ceram. Soc. Bull. 82 (11), 9701–9706.

Cass, R.B., Loh, R.R., Allen, T.C., 1998. Method for producing refractory filaments. US Patent No. 5,827,797.

Charnley, J., 1960. Anchorage of the femoral head prosthesis to the shaft of the femur. J. Bone Joint Surg. Br. 43B, 28–30.

Davies, J.P., O'Connor, D.O., Greer, J.A., Harris, W.H., 1987. Comparison of the mechanical properties of Simplex P, Zimmer Regular, and LVC bone cements. J. Biomed. Mater. Res. 21 (6), 719–730.

Gilbert, J.L., Ney, D.S., Lautenschlager, E.P., 1995. Self-reinforced composite poly(methyl methacrylate): static and fatigue properties. Biomaterials 16, 1043–1055.

Harper, E.J., Behiri, J.C., Bonfield, W., 1995. Flexural and fatigue properties of a bone cement based upon polyethylmethacrylate and hydroxyapatite. J. Mater. Sci., Mater. Med. 6 (12), 799–803.

Harper, E.J., Bonfield, W., 2000. Tensile characteristics of ten commercial acrylic bone cements. J. Biomed. Mater. Res. B 53 (5), 605–616.

Harper, E.J., Braden, M., Bonfield, W., 2000. Mechanical properties of hydroxyapatite reinforced poly(ethylmethacrylate) bone cement after immersion in a physiological solution: influence of a silane coupling agent. J. Mater. Sci., Mater. Med. 11 (8), 491–497.

Hoey, D., Taylor, D., 2009a. Quantitative analysis of the effect of porosity on the fatigue strength of bone cement. Acta Biomater. 5, 719–726.

Hoey, D., Taylor, D., 2009b. Statistical distribution of the fatigue strength of porous bone cement. Biomaterials 30, 6309–6317.

Kotha, S.P., Lieberman, M., Vickers, A., Schmid, S.R., Mason, J.J., 2006a. Adhesion enhancement of steel fibers to acrylic bone cement through a silane coupling agent. J. Biomed. Mater. Res. A 76, 111–119.

Kotha, S.P., Li, C., McGinn, P., Schmid, S.R., Mason, J.J., 2006b. Improved mechanical properties of acrylic bone cement with short titanium fiber reinforcement. J. Mater. Sci., Mater. Med. 17 (8), 1403–1409.

Kotha, S.P., Li, C., Schmid, S.R., Mason, J.J., 2004. Fracture toughness of steel-fiber-reinforced bone cement. J. Biomed. Mater. Res. A 70 (3), 514–521.

Kotha, S., Li, C., Schmid, S., Mason, J., 2009. Reinforcement of bone cement using zirconia fibers with and without acrylic coating. J. Biomed. Mater. Res. A 88 (4), 898–906.

Lennon, A.B., Prendergrast, P.J., 2001. Evaluation of cement stresses in finite element analyses of cemented orthopaedic implants. J. Biomech. Eng. 123, 623–628.

Lewis, G., 1997. Properties of acrylic bone cement: state of the art review. J. Biomed. Mater. Res. B 38 (2), 155–182.

Lewis, G., 2003. Fatigue testing and performance of acrylic bone–cement materials: state-of-the-art review. J. Biomed. Mater. Res. B 66 (1), 457–486.

Lewis, G., 2008. Alternative acrylic bone cement formulations for cemented arthroplasties: present status, key issues, and future prospects. J. Biomed. Mater. Res. B 84 (2), 301–319.

Lewis, G., 2009. Influence of powder-to-liquid monomer ratio on properties of an injectable iodine-containing acrylic bone cement for vertebroplasty and balloon kyphoplasty. J. Biomed. Mater. Res. B 91 (2), 537–544.

Lusti, H.R., Hine, P.J., Gusev, A.A., 2002. Direct numerical predictions for the elastic and thermoelastic properties of short fibre composites. Compos. Sci. Technol. 62, 1927–1934.

Martin, K.F., Davies, R.T., Rasiah, P.N., 1980. Axial fatigue strength of carbon fibre reinforced bone cement. J. Mech. Des. 102 (4), 723–726.

Matsuda, S., Kishi, H., Murakami, A., 2004. New processing of apatite fiber and some application for medical use. Compos. Sci. Technol. 64, 909–914.

Murray, D.W., Carr, A., Bulstrode, C.J., 1995. Which primary total hip replacement? J. Bone Joint Surg. Br. 77 (4), 520–527.

Pilliar, R.M., Blackwell, R., MacNab, I., Cameron, H.U., 1976. Carbon fiber-reinforced bone cement in orthopedic surgery. J. Biomed. Mater. Res. A 10 (6), 893–906.

Robinson, R.P., Wright, T.M., Burnstein, A.H., 1981. Mechanical properties of poly(methyl methacrylate) bone cements. J. Biomed. Mater. Res. A 15, 203–208.

Shen, H., Nutt, S., Hull, D., 2004. Direct observation and measurement of fiber architecture in short fiber-polymer composite foam through micro-CT imaging. Compos. Sci. Technol. 34, 2113–2120.

Toll, S., Andersson, P.-O., 1991. Microstructural characterization of injection moulded composites using image analysis. Composites 22 (4), 298–306.

Topoleski, L.D.T., Ducheyne, P., Cuckler, J.M., 1995. The effects of centrifugation and titanium fiber reinforcement on fatigue mechanisms in poly(methyl methacrylate) bone cement. J. Biomed. Mater. Res. A 29, 299–307.

Yue, W., Roeder, R.K., 2006. Micromechanical model for hydroxyapatite whisker reinforced polymer biocomposites. J. Mater. Res. 21 (8), 2136–2145.

Zhou, Y., Li, C., Mason, J.J., 2005. Shape optimization of randomly oriented short fibers for bone cement reinforcements. Mater. Sci. Eng. A 393 (1–2), 374–381.

Zhou, Y., Yue, W., Li, C., Mason, J.J., 2009. Static and fatigue mechanical characterizations of variable diameter fibers reinforced bone cement. J. Mater. Sci., Mater. Med. 20 (2), 633–641.

Zhu, Y.T., Beyerlein, I.J., 2002. Bone-shaped short fiber composites–an overview. Mater. Sci. Eng. A 326, 208–227.